Article

Evaluation of Future Streamflow in the Upper Part of the Nilwala River Basin (Sri Lanka) under Climate Change

Imiya M. Chathuranika [1], Miyuru B. Gunathilake [2], Hazi Md. Azamathulla [3] and Upaka Rathnayake [1,*]

1 Department of Civil Engineering, Faculty of Engineering, Sri Lanka Institute of Information Technology, Colombo 10115, Sri Lanka; imiyachathu@gmail.com
2 Hydrology and Aquatic Environment, Division of Environment and Natural Resources, Norwegian Institute of Bioeconomy and Research, 1433 Ås, Norway; miyuru.gunathilake@nibio.no
3 Department of Civil and Environmental Engineering, The Faculty of Engineering, The University of West Indies, St. Augustine 32080, Trinidad and Tobago; hazi.azamathulla@sta.uwi.edu
* Correspondence: upaka.r@sliit.lk; Tel.: +94-719883318

Abstract: Climate change is a serious and complex crisis that impacts humankind in different ways. It affects the availability of water resources, especially in the tropical regions of South Asia to a greater extent. However, the impact of climate change on water resources in Sri Lanka has been the least explored. Noteworthy, this is the first study in Sri Lanka that attempts to evaluate the impact of climate change in streamflow in a watershed located in the southern coastal belt of the island. The objective of this paper is to evaluate the climate change impact on streamflow of the Upper Nilwala River Basin (UNRB), Sri Lanka. In this study, the bias-corrected rainfall data from three Regional Climate Models (RCMs) under two Representative Concentration Pathways (RCPs): RCP4.5 and RCP8.5 were fed into the Hydrologic Engineering Center-Hydrologic Modeling System (HEC-HMS) model to obtain future streamflow. Bias correction of future rainfall data in the Nilwala River Basin (NRB) was conducted using the Linear Scaling Method (LSM). Future precipitation was projected under three timelines: 2020s (2021–2047), 2050s (2048–2073), and 2080s (2074–2099) and was compared against the baseline period from 1980 to 2020. The ensemble mean annual precipitation in the NRB is expected to rise by 3.63%, 16.49%, and 12.82% under the RCP 4.5 emission scenario during the 2020s, 2050s, and 2080s, and 4.26%, 8.94%, and 18.04% under RCP 8.5 emission scenario during 2020s, 2050s and 2080s, respectively. The future annual streamflow of the UNRB is projected to increase by 59.30% and 65.79% under the ensemble RCP4.5 and RCP8.5 climate scenarios, respectively, when compared to the baseline scenario. In addition, the seasonal flows are also expected to increase for both RCPs for all seasons with an exception during the southwest monsoon season in the 2015–2042 period under the RCP4.5 emission scenario. In general, the results of the present study demonstrate that climate and streamflow of the NRB are expected to experience changes when compared to current climatic conditions. The results of the present study will be of major importance for river basin planners and government agencies to develop sustainable water management strategies and adaptation options to offset the negative impacts of future changes in climate.

Keywords: climate change; Hydrologic Engineering Center-Hydrologic Modeling System (HEC-HMS); Representative Concentration Pathways (RCPs); streamflow; Upper Nilwala River Basin (UNRB)

1. Introduction

During the 20th and 21st centuries, the climate has been changing globally mainly due to anthropogenic activities. Increases in greenhouse gases such as carbon dioxide, methane, and nitrous oxide result in global warming [1,2] and thereby enhance the atmospheric evaporation demand [3,4]. Climate change is also identified as a critical environmental issue of the 21st century [5]. Extreme weather-caused environmental disasters have been reported during the last decade more frequently around the world [6]. Multiple studies

have been conducted to understand how the hydrological cycle has altered through the changes in climatic parameters such as precipitation and temperature [7–10]. Streamflow is a key element in the hydrological cycle, while water resources are invaluable for maintaining the sustainability of social, environmental, and economic systems [11–13]. Decrement in freshwater availability will negatively affect food production, irrigation, drinking water, industry, and hydropower production [14–16]. Therefore, assessing streamflow changes due to climate change is essential in both spatial and temporal scales. Many studies including Maharajan et al. [17], Shelton and Lin [18], Sirisena et al. [19], and Ghaderpour et al. [20] have conducted studies examining climate change impacts on river flow using different hydrologic models. These studies indicated that increases and decreases in precipitation and streamflow are expected in varying degrees in different locations of the world.

Surface water is withdrawn from rivers, lakes, tanks, etc., to fulfill the demands of many activities including agricultural, industrial, household, recreational, and power generation in Sri Lanka. Since ancient times, the lifestyles of most Sri Lankans were centered on agricultural activities. Most areas of the country were covered with agricultural crops including paddy, coconut, rubber, tea, cinnamon, etc. The construction of small, medium, and large tanks was initiated a long time ago to collect rainwater and stream water for cultivation purposes [21]. Hence, agriculture is considered a major economic sector in Sri Lanka since ancient times, and water resources are crucial to the development of Sri Lanka. These practices are continued until the present, with water being increasingly used in other sectors like hydropower production and construction as well [22].

Sri Lanka experiences a tropical monsoon climate zone that is influenced by two major monsoons [23]. The major rainfall seasons of the country are the southwest monsoon, the northeast monsoon, and the two inter-monsoon periods. The rainfall patterns of the country are strongly influenced by the direction of these monsoons [24]. The country's air temperature varies only slightly within the year, except in the central mountains due to changes in altitude [25]. Climate Risk Index (CRI) analysis ranked Sri Lanka within the top ten countries most affected by climate change in 2018 [26]. Extreme weather conditions were reported with higher magnitudes and frequencies during the last few decades due to climate change, and they caused many natural hazards including floods, droughts, cyclones, and landslides in the country [27,28]. Most of the rivers in Sri Lanka originate from the central highlands at an altitude of 2000 m above Mean Sea Level (MSL), and pass along the steep slopes in the upstream and mild slopes downstream before meeting the sea on the coast of the island following a radial draining system. Riparian zones in the upper parts of most of the drainage basins in Sri Lanka are intensely affected by anthropogenic activities such as deforestation, agriculture, urbanization, and industrialization. Understanding climate change patterns is essential for formulating plausible rainfall and temperature predictions [29–33].

Nilwala River Basin (NRB) is located in the wet zone and experiences some of the highest annual rainfall depths to the island [34]. Due to its geography and rainfall intensity in the upper parts, the downstream of the NRB experiences severe floods. As explained by Acharya et al. [35], drastic changes in rainfall will affect the hydrology of a river. Changes in timing and magnitude of the streamflow may also alter the flood behavior and distribution, water supply, recreational activities, agriculture, and water purification for drinking purposes. Drought conditions have been observed recently in some parts of the Matara district which has then resulted in water shortages for irrigation purposes [36]. Hence, crop patterns should be periodically changed for the plants to withstand the climatic conditions. The water in the Nilwala River is mainly used for drinking purposes by the people of the Matara district [37]. In addition, the water demand for the Nilwala River has increased due to the major development projects such as the southern expressway project, Matara-Beliatta railway track construction project, rural villages, and town development projects that have taken place rapidly in the southern province during the last two decades [38]. Seasonal precipitation changes adversely affect paddy, tea, rubber, and coconut cultivations in the southeast part of the NRB. Therefore, assessing the water availability under climate change

in the upper part of the NRB is important for decision-makers to take necessary actions to implement better water resources management practices. This study carries a significant amount of novelty since for the first time a climate change impact study was done for the NRB, which is located in the southern part of the country.

The impacts of climate change on streamflow have been least examined in the context of Sri Lanka using a modeling approach. According to the best understanding of the author, only Sirisena et al. [19] have attempted to examine the future climate impact on streamflow of the Kalu River Basin. The current study uses the Coordinated Regional Downscaling Experiment (CORDEX) regional climate data sets of 0.5° resolution for the first time for a river basin located in the Southern province of the island. Hence, this study provides a significant value to the scientific community by examining a river basin that experiences a coastal climate. The results of the present study will be of interest to many parties, including river basin planners and government agencies. The outcomes of the present study will aid to develop sustainable water management strategies and adaptation options to offset the negative impacts of future changes in climate expected in the NRB.

This study assesses the suitability of the Hydrologic Engineering Center-Hydrologic Modeling System (HEC-HMS) model in Upper Nilwala River Basin (UNRB) with objectives; (1) to analyze climate change in the future periods at the NRB, and (2) to investigate changes in the streamflow at UNRB due to climate change in the future timelines. The structure of the remaining parts of this paper includes material and methods, results, discussion, and conclusions.

2. Material and Methods

2.1. Study Area

The NRB is located in the southern end of the wet zone in Sri Lanka and it extends from latitude 5°55′ N to 6°13′ N and longitude 80°25′ E to 80°38′ E. The elevations range between −6 and 988 m above MSL. The watershed is surrounded by the Gin and Polwatta rivers on the western side and the Kirama and Urubokka Oya in the southern part. The NRB drains an area of 1010 km². The Nilwala River begins from Panilkanda in Deniyaya at an altitude of about 980 m above MSL, traverses about 72 km along different topographical zones passing Bopagoda, Akuressa, Kadduwa, and Matara urban areas, and falls into the sea at Thotamuna, Matara. The annual discharge through the Nilwala River into the Indian Ocean is more than 800 Million Cubic Meters (MCM). More than 70% of the watershed area is used for cultivation purposes mainly for paddy, tea, and rubber. Kotapola oya, Urubokke oya, Hulandaawa oya, Dhigili oya, Kirama oya and Siyabalagoda oya are some of the major tributaries of this river. Few tanks, such as Wilpita (Lenabatuwa or Haali-ela), Ellewela, and Kirama, were constructed for flood control and irrigation purposes. The location of the NRB is presented in Figures 1 and 2a, which show the land-use distribution for the study area.

Rainforests are the key land-use type in the UNRB, while tea, rubber, and home gardens also cover a significant land area. Annual precipitation is more than 3000 mm in the upper part of the NRB while around 1900 mm is received by the lower parts [34]. Usually, more rainfall is occurring during the northeast monsoon season (NMS; from December to February) and Second Inter Monsoon Season (IMS-2; from October and November). The other two climate seasons are First Inter Monsoon Season (IMS-1; from March to April) and southwest monsoon season (SWMS; from May to September). Higher elevated areas consist of reddish-yellow podzolic soils of which color varies from strong to yellowish-brown. The flat areas consist of Alluvium soils enriched with loose clay, sand, and clay, which can also be seen in intermediate and wet parts of Sri Lanka Bog and half-bog soils with color combinations of ash brown to black also can be seen in the lower part of the drainage basin [39]. Figure 2b depicts the soil distribution of the NRB according to the Digital Soil Map of the World (DSMW) soil classification [40].
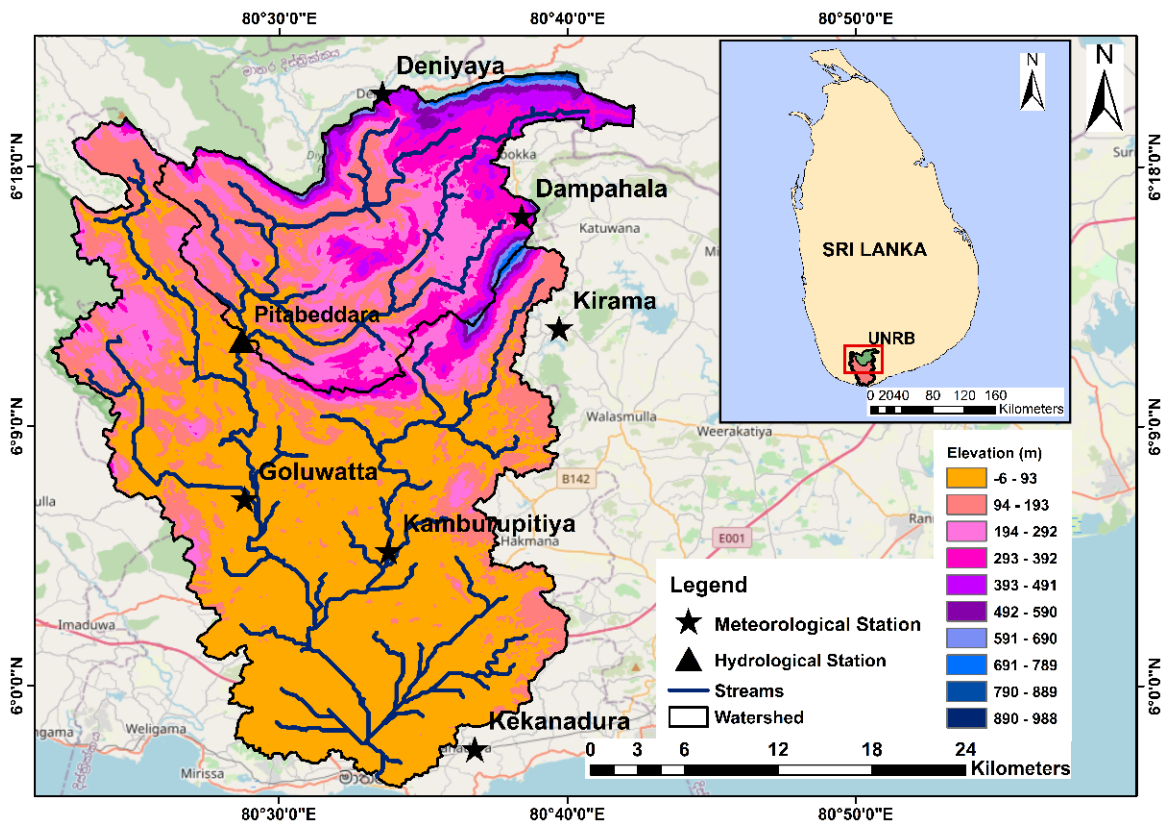
Figure 1. Location map of the Nilwala River Basin with its hydrological and meteorological stations.
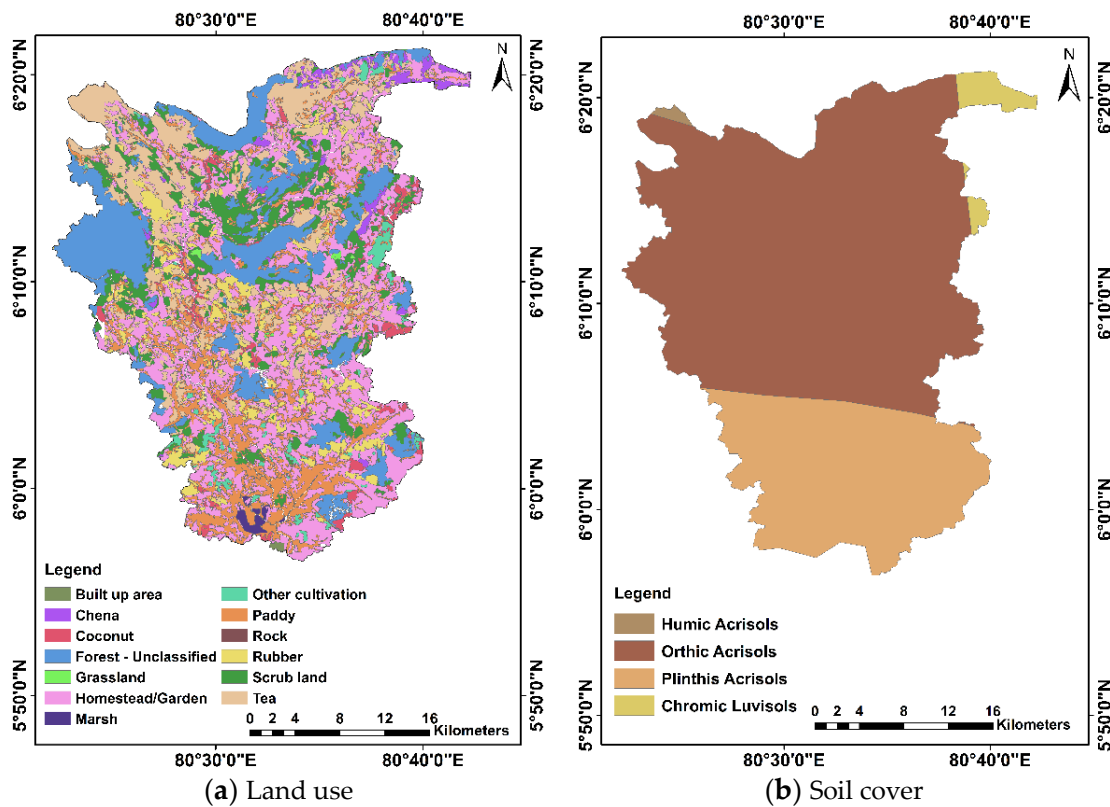

(**a**) Land use   (**b**) Soil cover

Figure 2. (**a**) Land use and (**b**) Soil maps of the Nilwala River Basin, Sri Lanka.

2.2. Data Collection

Daily observed discharge data at the Pitabeddara streamflow gauging station were collected from the Department of Irrigation of Sri Lanka from 1998 to 2014 (Refer to Figure 1). Observed daily precipitation data at Dampahala, Kamburupitiya, Kekenadura, Kirama, Goluwatta, and Deniyaya stations were collected from the Department of Meteorology of Sri Lanka for the years from 1980 to 2020. Observed streamflow at Pitabeddara station which is located upstream of the NRB was used for the HEC-HMS model development in this study due to the unavailability of data in a hydrological station that drains a larger area than that of Pitabeddara. The hydro-meteorological network used in this study is illustrated in Figure 1. The Digital Elevation Model (DEM) having a resolution of 30 m × 30 m was downloaded from Advanced Spaceborne Thermal Emission and Reflection Radiometer (ASTER). The land use data of the year 2012 was obtained from the Department of Survey in Sri Lanka for this study. Soil data was downloaded from the DSMW. DSMW vector data from the Food and Agriculture Organization (FAO) soils portal for South Asia was used and projected to WGS-1984 UTM Zone-44N coordinate system. The details of the hydro-meteorological stations used in the study are given in Table 1.

Table 1. Details of the hydro-meteorological stations in the NRB.

Station Name	Latitude °N	Longitude °E	Elevation above MSL (m)	Duration	
				From	To
Meteorological data					
Dampahala	6.27	80.64	176	1980	2020
Kamburupitiya	6.08	80.56	244	1980	2020
Kekenadura	5.97	80.57	49	1980	2020
Kirama	6.22	80.67	122	1980	2020
Goluwatta	6.10	80.48	16	1980	2020
Deniyaya	6.33	80.55	399	1980	2020
Hydrological data					
Pitabeddara	6.20	80.48	27	1998	2014

Apart from ground-based precipitation data, daily rainfall data from global gridded data such as Asian Precipitation-Highly Resolved Observational Data Integration towards Evaluation of Water Resources (APHRODITE) and can be extracted through (http://aphrodite.st.hirosaki-u.ac.jp/, accessed on 5 January 2022) [41]. These data have a resolution of 0.25° × 0.25° and are available for the period between 1998–2015. In addition, Precipitation Estimates from "Remotely Sensed Information using Artificial Neural Networks" (PERSIANN), "PERSIANN Cloud Classification System" (PERSIANN-CCS), and "PERSIANN Climate Data Record" (PERSIANN—CDR) were downloaded from the Center for Hydrometeorology and Remote Sensing (CHRS) data portals. The PERSIANN rainfall data was extracted from (https://chrsdata.eng.uci.edu/, accessed on 5 January 2022) [42]. PERSIANN, PERSIANN-CCS, and PERSIANN-CDR datasets are available from the years 2000, 2003, and 1983 with spatial and temporal resolutions of 0.25 and 1 h, 0.04 and 1 h and 0.25 and 1 h, respectively [43,44]. Due to the availability in the long-term run, these datasets can be used to perform long-term climate change analysis.

In the present study, the future rainfall in the NRB was simulated by three Regional Climate Models (RCMs) named ACCESS-SCIRO-CCAM (ACCESS), CNRM-CM5-CSIRO-CCAM (CNRM), and MPI-ESM-LR-CSIRO-CCAM (MPI) were downloaded from the South Asia Coordinated Regional Downscaling Experiment (CORDEX) data portal. These data were extracted from (https://cordex.org/, accessed on 5 January 2022) [10]. These climatic datasets have a 0.5° × 0.5° spatial resolution. Moreover, the extracted data represented two RCPs, namely, medium (RCP4.5) and high (RCP8.5) emission scenarios and a historical period spanning from 1980 to 2099. The details of the temporal and spatial datasets used in the study are illustrated in Table 2. Furthermore, the table provides information such as RCM developers, resolution, and a parent Global Climate Model (GCM).

Table 2. Temporal and spatial datasets used in the study.

Data	Reference	Resolution	Coverage
Topography (DEM)	[45]	30 m × 30 m	Global
APHRODITE rainfall	[41]	0.25°/daily	Monsoon Asia
Gridded rainfall	[42]	0.5°/daily	Global
RCMs (RCP4.5 and RCP8.5)	[10]		Global

RCM	Developer	Resolution	Parent GCM
ACCESS-CSIRO-CCAM	Collaboration for Australia Weather and Climate Research, Australian Government	0.5°/daily	ACCESS 1.0
CNRM-CM5-CSIRO-CCAM	National Centre for Meteorological Research	0.5°/daily	CNRM-CM5
MPI-ESM-LR-CSIRO-CCAM	European Network for Earth System Modelling	0.5°/daily	MPI-ESM-LR

2.3. Research Methodology

The scope of this study is to quantify the future climate of the NRB and identify its impact on the discharge of the UNRB at the Pitabeddara hydrologic station. This study also aims to assess the suitability of the HEC-HMS model for the study area. Yin et al. [46] stated that the mountain areas are more vulnerable to climate change. The potential impact of climate change on discharge at Pitabeddara is analyzed under three future timelines, namely, near future NF (2015–2042), mid future MF (2043–2070), and far future FF (2071–2099). The Linear Scale Method (LSM) bias correction is applied to adjust the biases prevailing in the climate data.

2.3.1. Filling Missing Climate Data

Accessing reliable quality data is the initial step for a hydro-meteorological study. Most meteorological stations are riddled with incomplete climate data, and this limits their usage for different studies. Instrumental errors, measurement errors, measurement location changes, changes in data collectors, measurement irregularity, and severe climate changes can cause an incomplete dataset. Numerous methods have been initiated to estimate missing data. These methods can be classified as empirical, statistical and function fitting approaches.

The percentages of missing data for each rainfall station in the NRB were calculated for Dampahala, Kekenadura, Goluwatta, Deniyaya, Kirama, and Kamburupitiya. These were 15.82%, 0.03%, 13.68%, 19.72%, 17.04%, and 18.09% for the 1980 to 2020 period. Hence, it was decided to use global precipitation data sets to fill the missing data in this study. Therefore, Satellite-Based Precipitation Products (SBPP) namely, PERSIANN, PERSIANN-CCS (CCS), and PERSIANN-CDR (CDR) were obtained to fill missing data after the distribution transformation bias adjustment method for the statistical downscaling climate model data. The distribution transformation approach determines the statistical distribution considering a time series for daily observed and SBPP datasets at the same station. Then, SBPP distribution is translated to the observed distribution and differences in the mean and variation are corrected. The correction factor for the mean and variation are given by Equations (1) and (2). Then, they were applied to adjust all pixels in the SBPP image by utilizing Equation (3) [47].

$$\mu_f = \frac{\mu_{OBS}}{\mu_{SBPP}} \tag{1}$$

$$\tau_f = \frac{\tau_{OBS}}{\tau_{SBPP}} \tag{2}$$

$$SBPP_C = (SBPP_0 - \mu_{SBPP}) \cdot \tau_f + \mu_{SBPP} \cdot \mu_f \tag{3}$$

where, μ_f, μ_{OBS}, μ_{SBPP}, τ_f, τ_{OBS}, τ_{SBPP}, $SBPP_C$ and $SBPP_0$ are the correction factor for the mean, the average value of observed data, the average SBPP, the correction factor for the variation, the standard deviation of observed data, the standard deviation of SBPP, the corrected SBPP, and the uncorrected SBPP, respectively.

Thereafter, the performance of the distribution transformation approach was evaluated using the percent bias (PBIAS), Root Mean Square Error (RMSE), and correlation coefficient (R) [14,48–50]. Afterward for the correction of SBPPs, an average was considered to fill the missing data by giving equal weight to each SBPP. For the time periods with missing data in which the SBPPs were unavailable APHRODITE daily rainfall data was used.

2.3.2. Future Climate Projection

Three RCM models of the Conformal Cubic Atmospheric Model (CCAM), which are ACCESS, CNRM, and MPI, were carefully selected based on their resolution, vintage, representativeness, and validity for this study [51]. It is mandatory to bias correct the outputs from selected RCMs. LSM was used for the bias correction at all meteorological stations under RCP4.5 and RCP8.5 climate scenarios [52]. The average monthly correction factors are found for precipitation with reference to the station-based precipitation data, and those historical scale factors are used for projecting future precipitation. Many studies have evaluated the performance of bias correction methods, concluding that the suitability of each bias correction method shows a relation to the location of the study area. Therefore, the performance of the bias correction was evaluated based on the statistics including Normalized Objective Function (NOF), PBIAS, and R.

Linear Scaling Method (LSM) is a simple, and widely used method for correcting biases in climatic datasets. Moreover, this method brings satisfactory results as the other complex techniques for coarse temporal scale analysis [53]. The Equations (4) and (5) are used for LSM for precipitation correction [54]. Future precipitation was analyzed annually, monthly, and seasonally [55]. These results are discussed in Section 3.1.

$$P_{his*}(d) = P_{his}(d) \times \left[\frac{\mu_m(P_{obs}(d))}{\mu_m(P_{his}(d))} \right] \tag{4}$$

$$P_{sim*}(d) = P_{sim}(d) \times \left[\frac{\mu_m(P_{obs}(d))}{\mu_m(P_{his}(d))} \right] \tag{5}$$

where, P, d, μ_m, *his*, *obs*, and *sim* are precipitation, daily, long term monthly mean, raw RCM hindcast, observed/measured data, and raw RCM forecast. The symbol * denotes the bias corrected datasets.

2.3.3. Hydrological Modelling

In this study, a widely used semi-distributed conceptual hydrological model, the HEC-HMS 4.6.1, which was developed by the United States Army Corps of Engineers, was used to simulate the rainfall-runoff processes. This hydrological model was previously used by Kim et al. [56], Gunathilake et al. [57], and many other hydrologists. The model calibration was carried out at daily time steps for 11 years from 1998 to 2008 in the present study. This long period contains distinct hydrologic regimes including wet, dry, and normal periods.

HEC-GeoHMS 10.2 and Arc-Hydro tools were used to create physical and hydrological characteristics/inputs that can be directly applied with HEC-HMS. The schematic representation of the watershed including sub-basins and streams were created by using these geospatial hydrology toolkits and the delineated map for the study area was used in the hydrological model. A one-parameter-at-a-time method was used for sensitivity analysis in which one parameter was held constant while the others were changed [58]. Manual calibration was conducted considering each sub-basin until a satisfactory match for each parameter was obtained between observed and simulated discharge. Moreover,

validation was done to test the model performance for a period of 6 years from 2009 to 2014. The goodness-of-fit statics considering monthly observed and simulated flows were also calculated to determine the model suitability for the determination of future streamflow at UNRB. In this study, the UNRB is considered up to the Pitabeddara hydrological station, which receives water from a 309 km^2 drainage area.

The HEC-HMS model set-up includes basin model, meteorological model, control specifications, and addition of time-series data [10]. The basin model includes the hydrologic element and their network of the movement of water through the river system of the study area. The meteorological component calculates the precipitation input spatially and temporally distributed over the watershed and this was carried out by the gauge weight method. Thiessen polygon method was used to find the gauge weights for precipitation inputs [59].

The presence of plants in the landscape is represented by the component canopy. Selecting a canopy is not compulsory, but this should be applied for continuous simulation processes. Three canopy methods named dynamic, simple, and gridded simple canopy are representing interception and evapotranspiration available in the HEC-HMS model. Canopy interception should be incorporated with an initial and constant method in continuous modeling. The simple canopy method was selected due to its compatibility with the loss method and usage for a continuous application.

The deficit and constant loss methods are similar to the initial and constant loss methods due to the usage of a single soil layer to calculate moisture content changes. The deficit and constant methods are widely used for continuous simulation processes with a canopy method. The number of parameters is also small compared to other loss methods available in HEC-HMS [60]. This method also takes account of the regain of initial loss after a long dry period without any rainfall event.

Clark unit hydrograph, Snyder's unit hydrograph, SCS_CN unit hydrograph, S curve, user-specified hydrograph, Modclark, and kinematic wave are the nine methods available in the HEC-HMS model to transform excess precipitation to runoff. Clark unit hydrograph method was used in this study due to the requirement of fewer parameters. This method also performed well compared to other transform methods in the optimization process. Time of concentration and storage coefficient are the input parameters for this method. The time needed for a water particle to travel from the most remote point to the watershed outlet is defined as the time of concentration. The storage coefficient (r) is an index of the temporary storage of rainfall surplus in the catchment as it flows to the outlet.

Direct runoff and baseflow are two distinct components in a hydrograph. Among the five baseflow methods available in HEC-HMS [61], baseflow for the UNRB was determined by the exponential recession method due to several reasons including due to capability of simulating continuous streamflow, less number of parameters, and the compatibility with the selected loss model. All the routing methods included in the HEC-HMS calculate a hydrograph downstream, given an upstream hydrograph as a boundary condition by solving the continuity and momentum equations. Muskingum model was selected for optimization, which includes a mass conservation method to route an inflow hydrograph.

All the methods used for the optimization of the HEC-HMS model were determined by examining each method until obtaining the best fit for observed and simulated monthly flow at Pitabeddara. Some of the initial values of model parameters were automatically calculated by the HEC-GeoHMS based on stream and basin characteristics [62]. Parameters were manually calibrated sub-basin wise when the required parameters were unable to estimate accurately for the UNRB.

2.3.4. Impact of Climate Change on Future Streamflow

Annual, monthly, and seasonal scales were used to analyze the impact of climate change on discharge at Pitabeddara compared to the baseline period from 1998 to 2014. The future period is divided into three timelines, NF (2015–2042), MF (2043–2070), and FF (2071–2099) in the study. In addition to that, Flow Duration Curves (FDCs) for future

timelines under RCP4.5 and RCP8.5 climate scenarios were also analyzed. Flow duration curve is another popular graphical tool that demonstrates the discharge that equaled or exceeded some percent of the time for a catchment or drainage area [63,64]. For more information about FDCs, readers are encouraged to refer to Ghaderpour et al. [20]. Therefore, the flood and drought conditions in the future period can be compared under different climate change scenarios by using FDCs at the Pitabeddara station for the future periods.

3. Results and Discussion

3.1. Future Climate Projection and Analysis

Missing data for six rainfall stations were calculated as stated in Section 2.3.1. The statistical performance of these SBPPs for each rainfall station is presented in Table 3. Calculated statistical indicators values are acceptable to fill the missing data. Then, bias correction using LSM was conducted for the three RCMs ACCESS, CNRM, and MPI under RCP4.5 and RCP8.5 emission scenarios for NF, MF, and FF periods as stated in Section 2.3. The statistical performance of LSM was determined before doing it for the future projections. Table 3 provides the results of the performance considering NOF, PBIAS, and RMSE of RCMs [65]. This was done by considering the mean observed and bias-corrected precipitation over the NRB.

Table 3. Results of the statistical performance of SBPP bias adjustment and LSM.

SBPP Bias Adjustment						
Statistical Indicator	Goluwatta	Dampahala	Kirama	Kamburupitiya	Kekenadura	Deniyaya
PBIAS	4.92	8.62	21.75	12.46	15.23	9.45
RMSE	5.26	6.14	4.56	4.38	3.72	7.20
r	0.49	0.58	0.59	0.55	0.54	0.60

LSM						
RCM	RCP4.5			RCP8.5		
	NOF	PBIAS	RMSE	NOF	PBIAS	RMSE
ACCESS	0.83	5.30	6.07	0.56	0.03	4.06
CNRM	0.87	3.76	6.36	0.84	9.43	6.14
MPI	1.17	29.39	8.51	0.90	19.25	6.54

Figure 3 demonstrates projected precipitation under RCP4.5 and RCP8.5 scenario from 2021 to 2099 and the precipitation during baseline period of 1980 to 2020 in NRB. The Thiessen–Mean method is used to calculate the mean precipitation over the NRB, and Box–Whisker diagrams of projected changes of precipitation with three RCMs for RCP4.5 and RCP8.5 scenarios are also demonstrated in Figure 3.

Ensembles were computed by considering an average by giving equal weights for each RCM as explained by Budhathoki et al. [66]. The precipitation is expected to increase throughout the period from 2021 to 2099 under RCP4.5 and RCP8.5. The projected minimum and maximum annual precipitations from CNRM are 1315.93 mm (in 2037) and 4821.63 mm (in 2063) whereas they are 1764.12 mm (in 2027) and 6353.82 mm (in 2054) for MPI. CNRM is projected to receive comparatively lower annual precipitations in the future compared to the baseline period for both RCP4.5 and RCP8.5 by showing 0.15% and 3.64% decrements, respectively. ACCESS and MPI provide increments under RCP4.5 of 12.19% and 20.63% and 11.95% and 22.7% under RCP8.5 for the future period with respect to the baseline period. Overall, ensembles for RCP4.5 are projected to rise by 3.63%, 16.49%, and 12.82%, whereas for RCP8.5 by 4.26%, 8.94%, and 18.04% for the 2020s, 2050s and 2080s compared to the baseline (for 1980–2020). MPI in the future period seems to have more wet years with respect to the reference period, including many extreme events, depicting a higher variability with higher intensities than the ACCESS and CNRM RCMs. Mean

and the median show an increment in the future, and it is an indication to receive more precipitations in the future period.
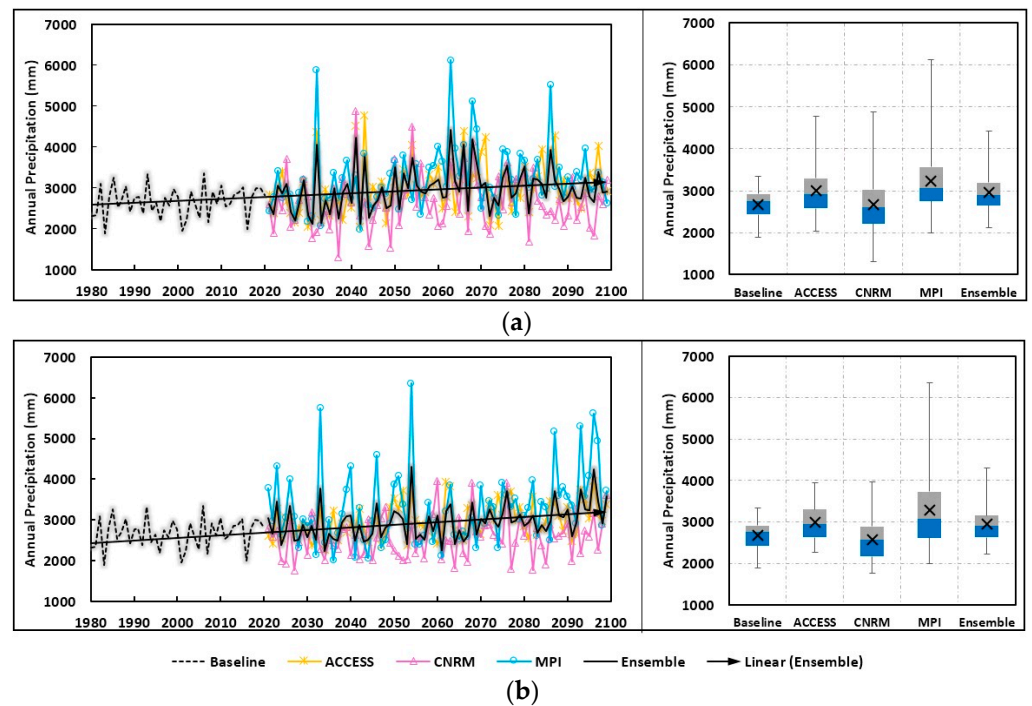

Figure 3. Projected precipitation under (**a**) RCP4.5 and (**b**) RCP8.5 climatic scenarios.

The trend analysis was carried out using the Mann–Kendall test and Sen's slope test for the ensembles precipitations. Increasing trends were found for both RCPs (4.9 mm/year for RCP4.5 and 63.9 mm/year for RCP8.5) under 5% confidence level.

The precipitation changes for the 2020s (2021–2047), 2050s (2048–2073), and 2080s (2074–2099) timelines in comparison with to baseline period (1980–2020) are given in Table 4. In the case of RCP4.5, MPI provides the highest precipitation change, amounting to 29.51% in the 2050s, and CNRM is forecasted to decrease by 4.61% in the 2020s. The same RCMs under RCP8.5 give a 35.82% maximum rise in the 2080s and a 7.37% minimum decrease in the 2020s. Ensembles showing increments in 2020s as 3.63%, 2050s as 16.49% and 2080s as 12.82% under RCP4.5 and in 2020s as 4.26%, 2050s as 8.94% and 2080s as 18.04% under RCP8.5.

Table 4. Change in precipitation (%) for three different time-lines and RCMs under RCP4.5 and RCP8.5 scenario compared to baseline period of 1980–2020 for Nilwala catchment.

RCM	RCP4.5			RCP8.5		
	2020s	2050s	2080s	2020s	2050s	2080s
ACCESS	5.80	15.82	15.19	3.66	13.62	18.90
CNRM	−4.61	4.15	0.17	−7.37	−2.82	−0.59
MPI	9.70	29.51	23.10	16.47	16.03	35.82
Ensemble	3.63	16.49	12.82	4.26	8.94	18.04

Figure 4 illustrates the mean monthly precipitation over the NRB for the 2020s, 2050s, and 2080s under the two emission scenarios with respect to the reference period. Generally, the highest rainfalls are received in October, November, and December compared to other months for all RCMs under both RCPs. Moreover, the peak rainfall is expected in November except for MPI, which has a maximum rise in October for the 2020s under RCP4.5. The rainfall projections from MPI confirm that it will receive maximum peaks in 2080s November, amounting to 585.16 mm and 719.40 mm under RCP4.5 and RCP8.5,

respectively. The June, July, and August months are expected to receive lower precipitations under all climate scenarios.
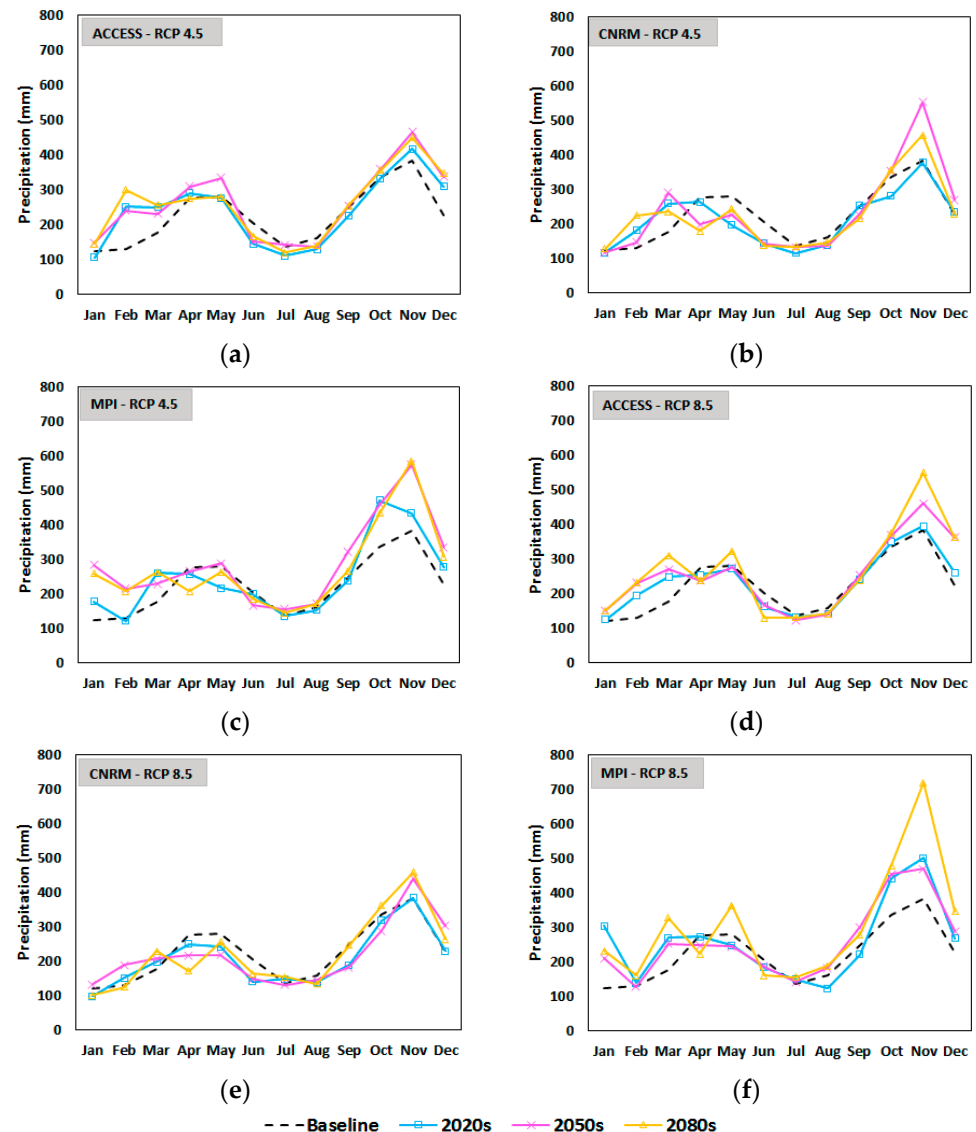

Figure 4. Monthly projected precipitation of NRB for 2020s, 2050s and 2080s under RCP4.5 and RCP8.5 scenarios compared with the baseline (1980–2020). (**a**) For ACCESS—RCP4.5, (**b**) for CNRM—RCP4.5, (**c**) for MPI—RCP4.5, (**d**) for ACCESS—RCP8.5, (**e**) for CNRM—RCP8.5, and (**f**) for MPI—RCP8.5.

Figure 5 depicts the seasonal precipitation in the NRB under different climate scenarios. Most of the area of the NRB is allocated for agricultural purposes, especially paddy cultivation. Therefore, the seasonal changes in precipitation are essential to identify the growing/harvesting periods for paddy cultivation seasons in the future periods. Minimum and maximum seasonal precipitations changes under RCP4.5 are expected to be a decrement of 17.77% during SWMS and an increment of 75.13% during NMS. These changes will be for CNRM in the 2020s and MPI in the 2050s. The SWMS season gives a maximum decrement of 19.89% by CNRM in the 2050s, and IMS-2 is projected to have a maximum rise of 66.91% by MPI in the 2080s compared to the baseline period.
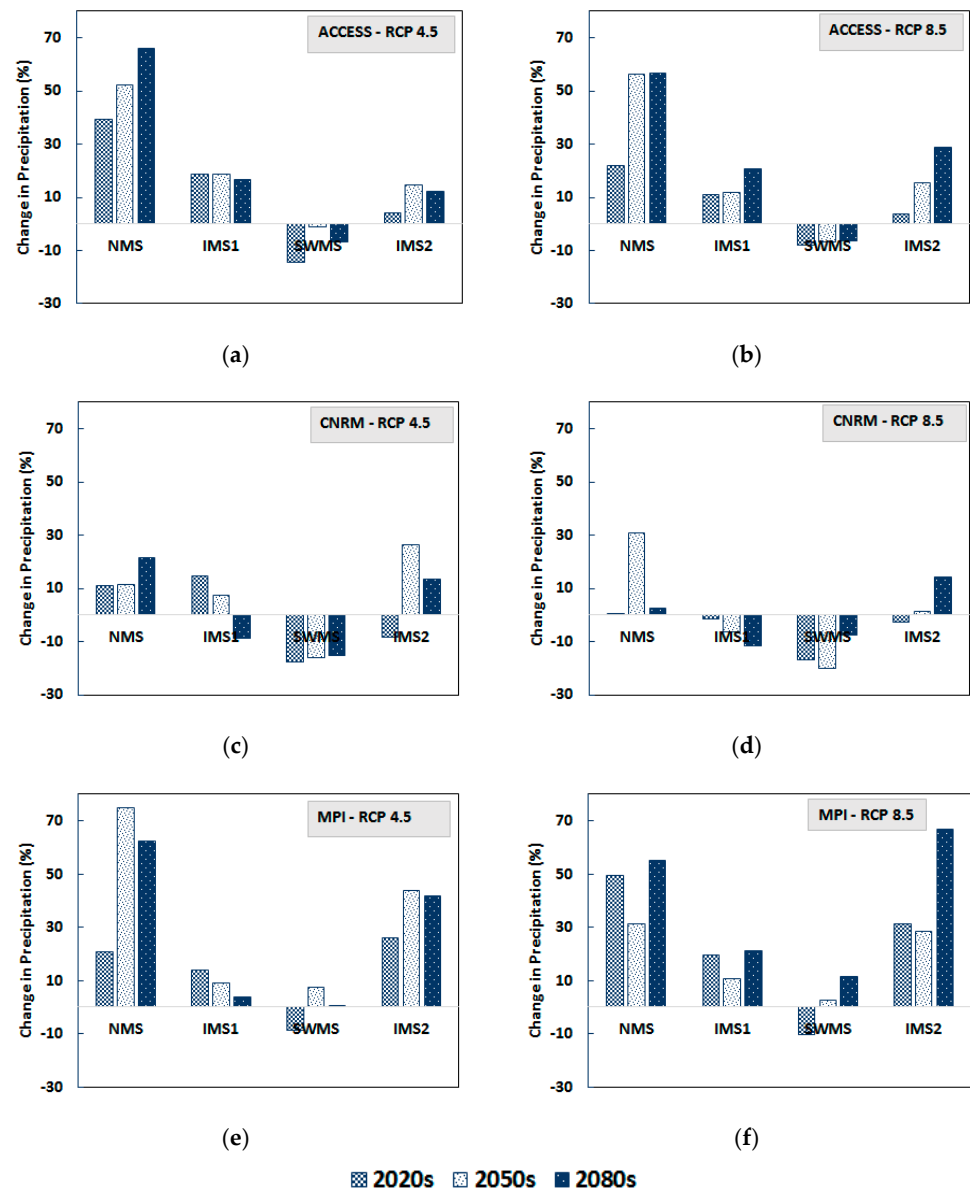
Figure 5. Seasonal change in precipitation in different periods for three RCMs ACCESS, CNRM and MPI under RCP4.5 and RCP8.5 in Nilwala watershed. (**a**) For ACCESS-RCP4.5, (**b**) for ACCESS-RCP8.5, (**c**) for CNRM-RCP4.5, (**d**) for CNRM-RCP8.5, (**e**) for MPI-RCP4.5, and (**f**) for MPI-RCP8.5.

3.2. Calibration of the HEC-HMS Model

Through the sensitivity analysis, the parameters controlling the watershed's hydrology were found to be constant rate, impervious percentage, time of concentration, storage coefficient, recession constant, ratio to peak, and Muskingum K. The catchment outlet of UNRB is taken as the Pitabeddara hydrological station due to unavailability of a downstream flow measuring station in NRB. According to Section 2.3.3, the baseline period was selected as the 1998–2014 period due to the availability of streamflow records during this particular duration. In this study, a daily time-step was used to simulate streamflow at Pitabeddara for future periods under different climate scenarios. The statistical indicators including Nash-Sutcliffe Efficiency (NSE), NOF, PBIAS, and R were calculated considering observed and simulated monthly discharge at Pitabeddara. Table 5 provides the hydrological model performance for the UNRB for the calibration and validation periods. As seen from the statistical values obtained the calibrated HEC-HMS model is acceptable to simulate streamflow at Pitabeddara in UNRB. The results from calibration and validation provide lesser

values for PBIAS and NOF meanwhile giving higher values within 0.50 to 0.84 for R and NSE. Moreover, the NSE values of 0.50 and 0.69 are 'satisfactory' and 'good' according to the model classification proposed by Moriasi et al. [67]. Furthermore, Pbias of 5.76% and 6.52% are deemed to be 'very good' according to the same classification.

Table 5. HEC-HMS model performance at Pitebaddera hydrologic station.

Statistical Indicator and Time	NOF	NSE	PBIAS	R
Calibration (1998–2008)	0.43	0.5	5.76	0.74
Validation (2009–2014)	0.36	0.69	6.52	0.84

The values of the calibrated parameters which are optimized in the HEC-HMS model development for the UNRB are given in Table 6.

Table 6. Optimized parameters and their values in the HEC-HMS model.

| Method	Parameter/Units	Optimized Value
Simple canopy	Initial storage (%)	20%
	Max storage (mm)	10
	Crop coeffient	1
Deficit and constant	Initial deficit (mm)	10
	Max storage (mm)	45
	Constant rate	1.2
	Impervious (%)	42–55
Clark unit hydrograph	Time of concentration (h)	24
	Storage coefficient (h)	22–66
Recession baseflow	Initial discharge (m^3/s)	0.23
	Recession constant	0.85–0.91
	Ratio to peak	0.22–0.26
Muskingum routing	K (hr)	0.7
	X	0.3

The hydrographs for observed and simulated monthly discharge for calibration and validation periods are illustrated in Figure 6. Minimal variability can be seen in peak flows while the baseflow is well captured by the HEC-HMS model. The highest peaks of the simulated streamflows are captured at an acceptable level, during the months of higher rainfall events occurring in both calibration and validation processes. However, mismatches were observed for a few events.

Therefore, these visual and statistical performances demonstrate that the developed HEC-HMS model is capable to capture the monthly streamflow of the UNRB. However, some simulated peaks show slight lags.

3.3. Impact of Climate Change in Future Streamflow

Figure 7 depicts the trends of future streamflows until 2099 at Pitabeddara station under RCP4.5 and RCP8.5 for all three RCMs and also for the ensemble case. All RCMs under both RCP scenarios show a continuous increasing trend in the future period similar to the baseline period of 1998–2014. Significant variability in annual streamflow can be noticed in the future, compared to the reference period at Pitabeddara. Ensembles show a maximum decrease and a significant rise in annual streamflow in 2016 as 4071.97 m^3/s and in 2063 as 16179 m^3/s under RCP4.5 and the same under RCP8.5 is projected to receive in 2016 as 4083 m^3/s and in 2096 as 14984 m^3/s. The annual discharge at Pitabeddara is projected to increase until the end of 2099 by 59.30% and 65.79% under RCP4.5 and RCP8.5 emission scenarios compared to the baseline period. During the reference period (1998–2014) the mean annual water volume was calculated to be 500.73 Million Cubic Meters (MCM) at Pitabeddara. The annual water volume is expected to rise in the 2020s

by 24.66%, 2050s by 68.60%, and 2080s by 59.30% under RCP4.5 for the ensemble scenario. The increments are by 27.32% in the 2020s, 46.04% in the 2050s, and 65.80% in the 2080s by under RCP8.5, respectively. Currently, lower parts at NRB face floods, and these increments in water availability at Pitabeddara show more flood hazards in the future.
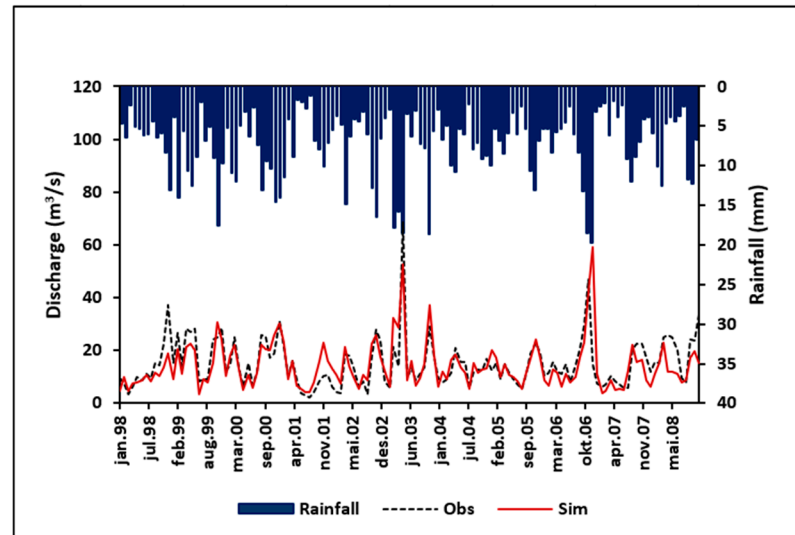
(**a**)
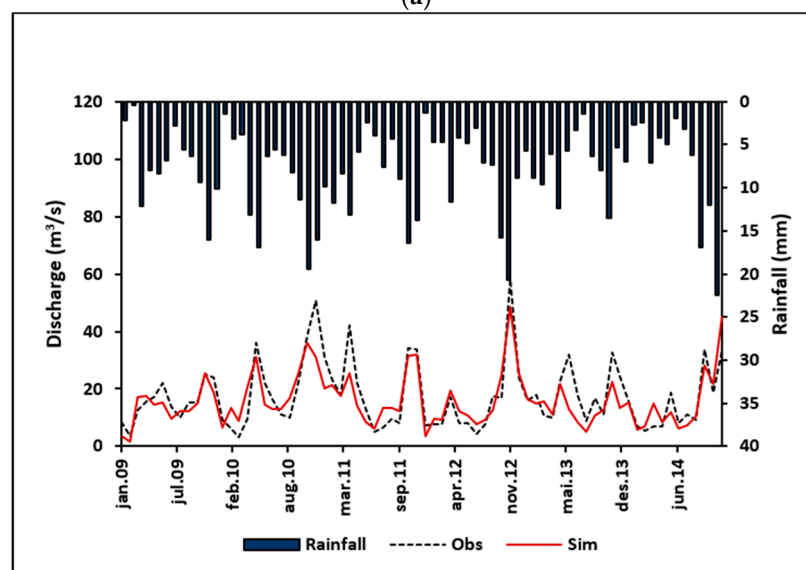
(**b**)

Figure 6. Observed and simulated monthly hydrograph comparison (**a**) for calibration and (**b**) for validation at the Pitabeddara hydrological station.
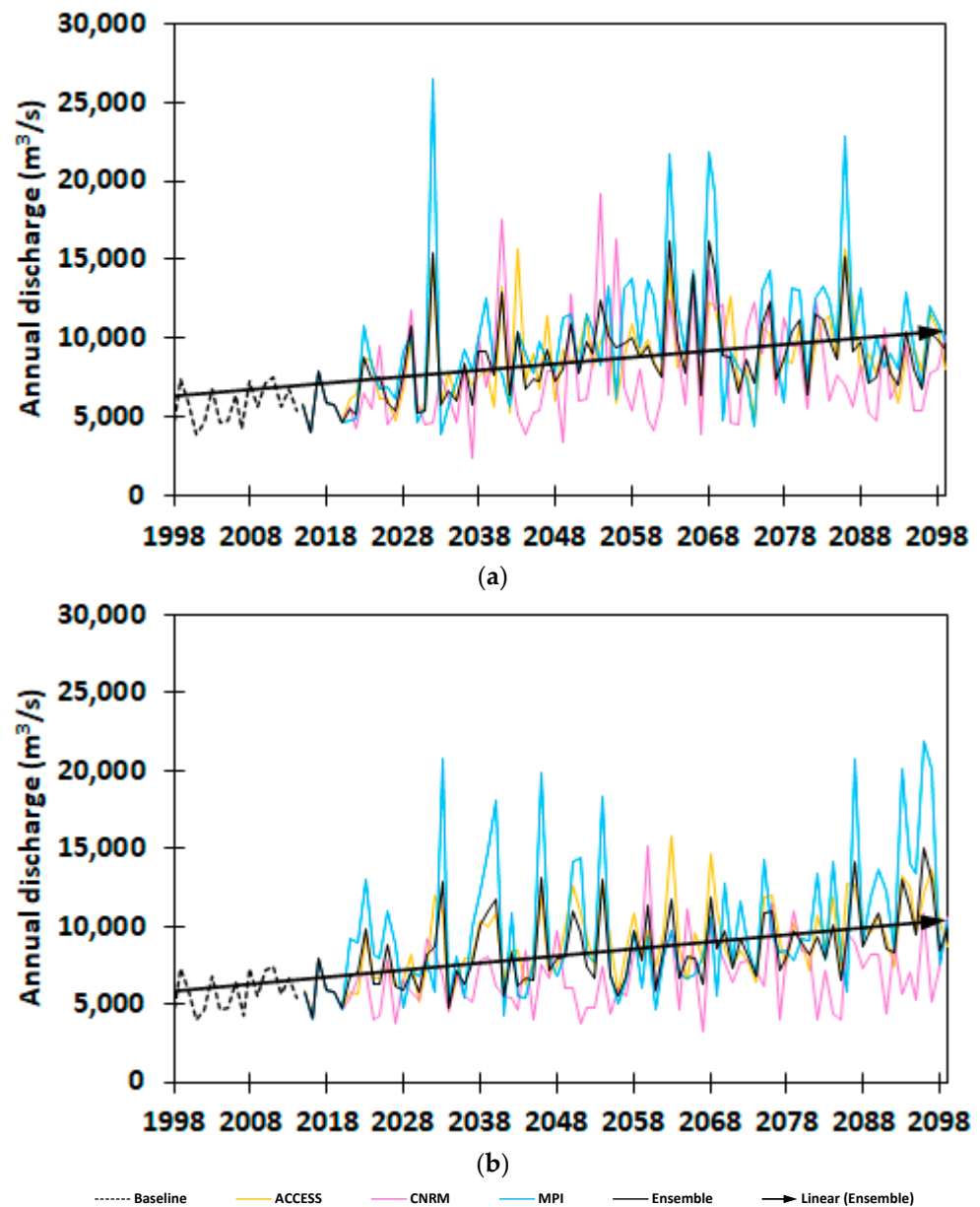
Figure 7. Projected annual discharge at Pitabaddara under (**a**) RCP4.5 and (**b**) RCP8.5 for ACCESS, CNRM and MPI RCMs.

In addition, non-parametric trend analysis using the Mann–Kendall test and Sen's slope estimator test have showcased increasing trends in streamflows. 4.9 m^3/s/year and 6.9 m^3/s/year were observed for both projected streamflows from RCP4.5 and RCP8.5, respectively. The same pattern can be observed in the projected rainfalls. This is understandable as rainfall is the main driving factor for the streamflow.

As stated in Section 2.3.3 in order to analyze monthly and seasonal streamflows in the future period, the future period is divided into three different timelines. They are Near Future (NF) (2015–2042), Middle Future (MF) (2043–2070), and Far Future (FF) (2071–2099). Projected mean monthly streamflows at Pitabeddara station for ACCESS, CNRM, and MPI under RCP4.5 and RCP8.5 climate scenarios are plotted in Figure 8 with respect to the baseline period (1998–2014). The simulated ensemble streamflow for the NF, MF, and FF under the RCP4.5 scenario demonstrated a peak in November with values of 36.95 m^3/s, 58.99 m^3/s, and 54.85 m^3/s while showing maximum decrement in July for NF and FF demonstrating 8.85 m^3/s and 11.95 m^3/s except in August as 11.07 m^3/s in MF. The maxi-

mum increase in mean monthly ensemble discharge is recorded in November for NF, MF, and FF as 38.93 m^3/s, 48.12 m^3/s, and 68.15 m^3/s under RCP8.5, and maximum decrease is provided for NF, MF, and FF as 9.25 m^3/s, 12.03 m^3/s and 11.87 m^3/s in August, June and July, respectively. There are higher mean monthly streamflows (approximately 20 m^3/s higher) recorded under both RCPs. It can be observed that when comparing individual RCMs, under RCP4.5 and RCP8.5, higher mean monthly streamflows are expected to be received in October, November, and December compared to other months during each timeline.
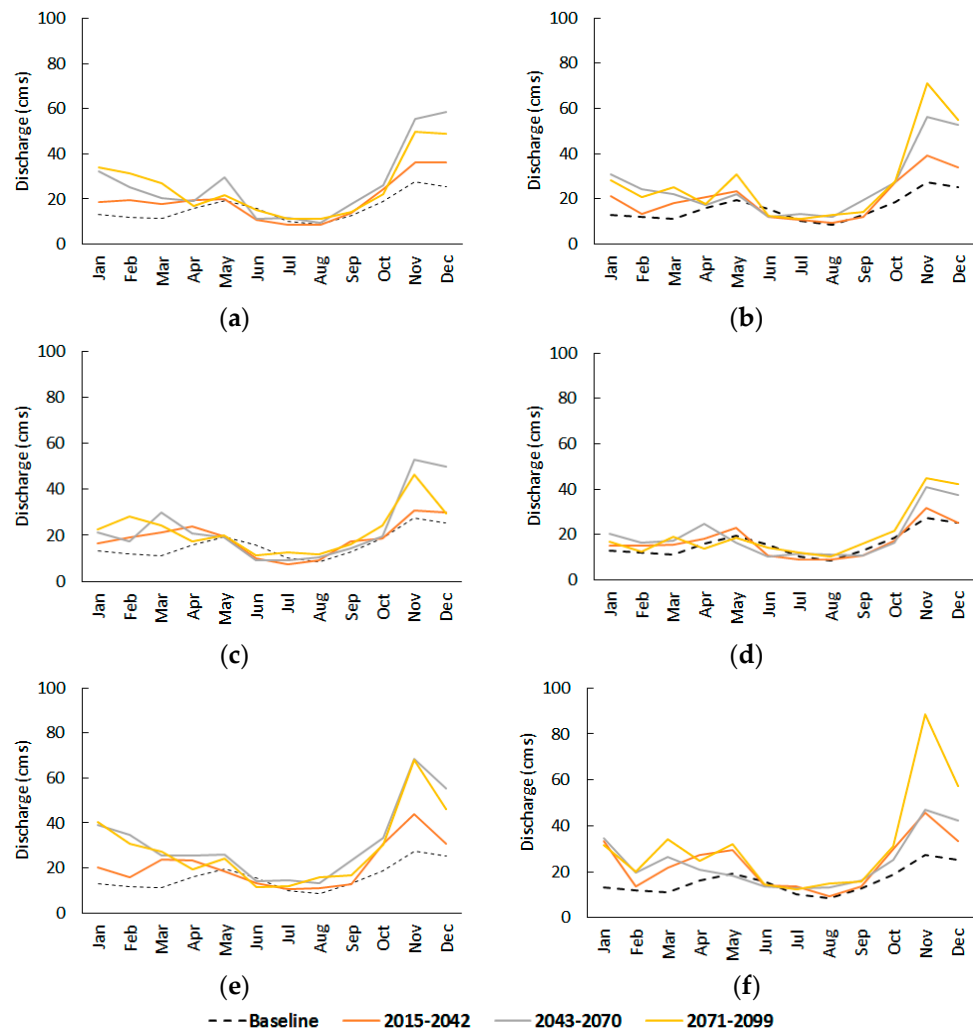

Figure 8. Future mean monthly discharge for near (2015–2042), mid (2043–2070) and far (2071–2099) under RCP4.5 and RCP8.5 scenario compared with the baseline period (1998–2014), (**a**) for ACCESS—RCP4.5, (**b**) for ACCESS—RCP8.5, (**c**) for CNRM—RCP4.5, (**d**) for CNRM—RCP8.5, (**e**) for MPI—RCP4.5, and (**f**) for MPI—RCP8.5.

Analyzing seasonal streamflow is very useful for agricultural professionals in the NRB to obtain insights to implement land preparation, crop establishment, and water/nutrient management practices. The NRB experiences four rainfall seasons, which are NMS, IMS-1, SWMS, and IMS-2, as expressed in Section 2.1 of this paper. Typically, IMS-2 and NMS seasons are representing the wet season while the other two seasons IMS-1 and SWMS are dry seasons. The seasonal changes of streamflows based on seasonal rainfalls can be clearly seen from Table 7 for both RCPs. Streamflow variation is depending on the season. Projected mean streamflows on a seasonal basis are analyzed based on the aforementioned four seasons. The highest increase of seasonal streamflow changes under RCP4.5 is 156.59% in MPI. Similarly, the highest increase under RCP8.5 is 159.19% in MPI during the IMS-2.

The city of Matara, which was prone to floods during the last few decades, is likely to experience further flooding in the future during NMS and IMS-2 seasons as streamflows are expected to increase.

Table 7. Projected mean seasonal changes (%) in streamflow for NF (2015–2042), MF (2043–2070) and FF (2071–2099) at Pitabeddara compared with the baseline period (1998–2014) under RCP4.5 and RCP8.5 scenarios in the UNRB.

Period	RCM	RCP4.5				RCP8.5			
		NMS	IMS-1	SWMS	IMS-2	NMS	IMS-1	SWMS	IMS-2
NF	ACCESS	47.76	37.00	−7.37	30.44	35.99	42.77	1.46	44.20
	CNRM	31.15	65.88	−4.86	7.50	9.77	24.19	−7.35	5.74
	MPI	32.46	72.94	−0.74	61.61	60.25	79.61	20.31	62.91
MF	ACCESS	131.30	43.84	19.12	76.65	114.30	43.88	17.79	81.26
	CNRM	76.84	86.30	−7.08	56.82	48.07	54.25	−9.32	23.67
	MPI	156.59	87.72	36.82	120.34	92.49	74.15	11.72	56.26
FF	ACCESS	127.49	60.16	10.58	55.99	107.52	56.44	21.18	114.00
	CNRM	59.79	52.97	6.94	53.61	41.76	20.78	6.06	43.85
	MPI	134.25	71.16	21.18	112.91	117.29	116.82	34.95	159.19

NMS-Northeast Monsoon Season; IMS-1-First Inter Monsoon Season; SWMS-Southwest Monsoon Season; IMS-2-Second Inter Monsoon Season.

Low flows (more than 95% of exceedance) and high flows (between 0–25% exceedance) are demonstrated through the FDCs at Pitabeddara station considering ensemble daily flows under RCP4.5 and RCP8.5 emission scenarios in the NF, MF, and FF from Figure 9. Compared to the baseline, high flows are projected to increase for NF, MF, and FF as 24.18%, 78.28%, and 60.28% under RCP4.5 and as 27.74%, 46.65%, and 71.72% under RCP8.5. Low flows are expected to increase for NF, MF, and FF by 11.26%, 88.74% and 93.07% under RCP4.5 and by 12.55%, 104.33%, and 125.97% under the RCP8.5 scenario. Therefore, severe flood and drought conditions are expected in MF and FF periods under both RCPs.
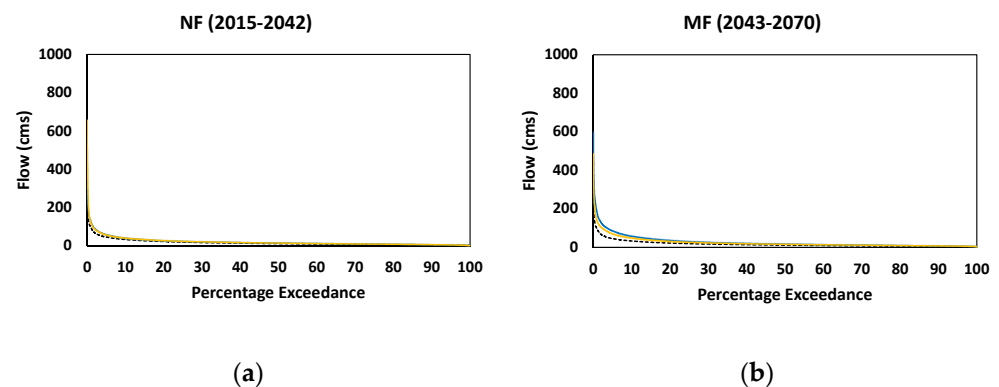

(**a**)
(**b**)
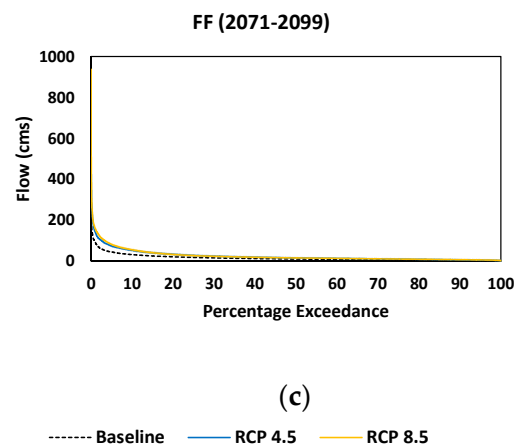
Figure 9. *Cont.*

Figure 9. Flow duration curves at Pitabeddara hydrological station under baseline, RCP4.5 and RCP8.5 in (**a**) NF, (**b**) MF and (**c**) FF periods.

3.4. Uncertainties and Limitations of the Study

It is noteworthy that the results of the present study demonstrated a significant uncertainty in terms of future rainfall and streamflow projections in the NRB. For instance, the rainfall projections obtained from ACCESS and MPI demonstrate increases in future seasonal and annual rainfall while for CNRM it is negative for most of the time horizons considered. These results agree with the findings of Gunathilake et al. [10] who assessed the future climate on tropical Upper Nan River Basin in Northern Thailand. Moreover, simulated streamflow rates are much higher for RCP 8.5 when compared to RCP 4.5 obtained through the present study. Natural variations in the earth, including El-Nino and La-Nina impacts, will add a significant source of uncertainty in future climates of the NRB of Sri Lanka.

4. Conclusions

The main objective of the study was to assess the climate change impact on the streamflow in the upper part of the Nilwala catchment in Sri Lanka. The climate change for the future period was analyzed for the NRB under RCP4.5 and RCP8.5 emission scenarios by using three bias-corrected RCMs namely ACCESS, CNRM, and MPI. The semi-distributed HEC-HMS model was selected for hydrological modeling. There were significant variations in the future annual precipitation in each RCM. The ensembles show an increasing trend during the periods of 2020s, 2050s, and 2080s with increases of 3.63%, 16.49%, and 12.82% under RCP4.5 and 4.26%, 8.94%, and 18.04% under RCP 8.5 emission scenarios compared to the baseline period between 1980–2020. Future streamflow at Pitabeddara was found to be increased by 59.3% and 65.79% under RCP4.5 and RCP8.5 until the end of 2099. IMS-2 and NMS seasons are expected to receive more rainfall than the reference period, therefore the streamflow at Pitabeddara is projected to receive high flows during those seasons. More floods and drought conditions are expected during the future period. Therefore, there is a need to construct storage within the UNRB. By building storage facilities, flooding can be reduced and the collected water can be supplied for many sectors during drought periods in the future. It's important to activate sustainable water management practices throughout the study area, which is a timely requirement to adapt to climate change.

Hydrological modelling outputs are subject to the uncertainty resulting from different sources of errors (e.g., error in input data, model structure, and model parameters). Moreover, the model simplification process can also lead to model uncertainties. A limitation of the present study is that the land-use changes during the study period were not taken into account. Bias-corrected climate data and HEC-HMS model calibration can have many uncertainties. Therefore, it is recommended to use different methods of other bias correction methods considering other RCMs for South Asia and add land-use changes with future development works in the study area for the prediction of streamflow in the future period.

Other hydrological models, such as Soil & Water Assessment Tool (SWAT) [68,69], Water Evaluation And Planning System (WEAP) [70] MIKE SHE [71] etc., are recommended to use for the study area to compare with HEC-HMS. Moreover, as a part of a future study, it is recommended to use the JUST and LSWAVE package, which can provide coherency and phase differences results in the time-frequency domain for streamflow and precipitation [72,73]. This is important for water resources/irrigation planners, agricultural professionals, and policymakers to supply water in a sufficient way for irrigation practices, drinking water purposes, domestic and industrial uses for the downstream areas in the NRB. This would also help to get an idea regarding flood and drought situations in the future period.

Author Contributions: Conceptualization, I.M.C. and M.B.G.; methodology, I.M.C.; software, I.M.C.; validation, I.M.C.; formal analysis, I.M.C. and M.B.G.; resources, U.R. and M.B.G.; data curation, U.R.; writing—original draft preparation, I.M.C.; writing—review and editing, I.M.C., M.B.G., U.R. and H.M.A.; supervision, M.B.G. and U.R.; project administration, U.R.; funding acquisition, U.R. All authors have read and agreed to the published version of the manuscript.

Data Availability Statement: Data used in this research can be requested from the corresponding author for research purposes.

Conflicts of Interest: The authors declare no conflict of interest.

References

1. IPCC. Summary for policymakers. In *Climate Change 2014: Impacts, Adaptation, and Vulnerability. Part A: Global and Sectoral Aspects. Contribution of Working Group II to the Fifth Assessment Report of the Intergovernmental Panel on Climate Change*; Cambridge University Press: Cambridge, UK; New York, NY, USA, 2014.
2. Ahiablame, L.; Sinha, T.; Paul, M.; Ji, J.-H.; Rajib, A. Streamflow response to potential land use and climate changes in the James River watershed, Upper Midwest United States. *J. Hydrol. Reg. Stud.* **2017**, *14*, 150–166. [CrossRef]
3. Eliades, M.; Bruggeman, A.; Lubczynski, M.W.; Christou, A.; Camera, C.; Djuma, H. The water balance components of Mediterranean pine trees on a steep mountain slope during two hydrologically contrasting years. *J. Hydrol.* **2018**, *562*, 712–724. [CrossRef]
4. Wang, K.; Liang, S. Global atmospheric downward longwave radiation over land surface under all-sky conditions from 1973 to 2008. *J. Geophys. Res.* **2009**, *114*, 1–12. [CrossRef]
5. Vargas-Amelin, E.; Pindado, P. The challenge of climate change in Spain: Water resources, agriculture and land. *J. Hydrol.* **2014**, *518*, 243–249. [CrossRef]
6. Lee, C.-H.; Yeh, H.-F. Impact of climate change and human activities on streamflow variations based on the Budyko framework. *Water* **2019**, *11*, 2001. [CrossRef]
7. Raneesh, K.Y.; Santosh, G.T. A study on the impact of climate change on streamflow at the watershed scale in the humid tropics. *Hydrol. Sci. J. J. Des Sci. Hydrol.* **2011**, *56*, 946–965. [CrossRef]
8. Dahal, N.; Shrestha, U.; Tuitui, A.; Ojha, H. Temporal changes in precipitation and temperature and their implications on the streamflow of Rosi river, Central Nepal. *Climate* **2019**, *7*, 3. [CrossRef]
9. Vandana, K.; Islam, A.; Sarthi, P.P.; Sikka, A.K.; Kapil, H. Assessment of potential impact of climate change on streamflow: A case study of the Brahmani River basin, India. *J. Water Clim. Chang.* **2019**, *10*, 624–641. [CrossRef]
10. Gunathilake, M.B.; Amaratunga, Y.V.; Perera, A.; Chathuranika, I.M.; Gunathilake, A.S.; Rathnayake, U. Evaluation of future climate and potential impact on streamflow in the Upper Nan River Basin of Northern Thailand. *Adv. Meteorol.* **2020**, *2020*, 1–15. [CrossRef]
11. Liu, Z.; Cuo, L.; Li, Q.; Liu, X.; Ma, X.; Liang, L.; Ding, J. Impacts of climate change and land use/cover change on streamflow in Beichuan River Basin in Qinghai province, China. *Water* **2020**, *12*, 1198. [CrossRef]
12. Masud, M.B.; Soni, P.; Shrestha, S.; Tripathi, N.K. Changes in climate extremes over North Thailand, 1960–2099. *J. Climatol.* **2016**, *2016*, 1–18. [CrossRef]
13. Gao, D.; Chen, T.; Yang, K.; Zhou, J.; Ao, T. Projecting the impacts of climate change on streamflow in the upper reaches of the Yangtze River basin. *J. Water Clim. Chang.* **2021**, *12*, 1724–1743. [CrossRef]
14. Navas, R.; Alonso, J.; Gorgoglione, A.; Vervoort, R. Identifying climate and human impact trends in streamflow: A case study in Uruguay. *Water* **2019**, *11*, 1433. [CrossRef]

15. Gunawardana, S.K.; Shrestha, S.; Mohanasundaram, S.; Salin, K.R.; Piman, T. Multiple drivers of hydrological alteration in the transboundary Srepok River Basin of the Lower Mekong Region. *J. Environ. Manag.* **2021**, *278*, 1–11. [CrossRef] [PubMed]

16. Yilmaz, A.G.; Atabay, S.; Amou-Assar, K.H.; Imteaz, M.A. Climate change impacts on inflows into lake Eppalock reservoir from Upper Campaspe catchment. *Hydrology* **2021**, *8*, 108. [CrossRef]

17. Maharjan, M.; Aryal, A.; Talchabhadel, R.; Thapa, B.R. Impact of climate change on the streamflow modulated by changes in precipitation and temperature in the north latitude watershed of Nepal. *Hydrology* **2021**, *8*, 117. [CrossRef]

18. Shelton, S.; Lin, Z. Streamflow variability in Mahaweli river basin of Sri Lanka during 1990–2014 and its possible mechanisms. *Water* **2019**, *11*, 2485. [CrossRef]

19. Sirisena, T.A.; Maskey, S.; Bamunawala, J.; Coppola, E.; Ranasinghe, R. Projected streamflow and sediment supply under changing climate to the coast of the Kalu river basin in tropical Sri Lanka over the 21st century. *Water* **2021**, *13*, 31. [CrossRef]

20. Ghaderpour, E.; Vujadinovic, T.; Hassan, Q.K. Application of the least-squares wavelet software in hydrology: Athabasca River basin. *J. Hydrol. Reg. Stud.* **2021**, *36*, 1–18. [CrossRef]

21. Abeywardana, N.; Bebermeier, W.; Schütt, B. Ancient water management and governance in the dry zone of Sri Lanka until abandonment, and the influence of colonial politics during reclamation. *Water* **2018**, *10*, 1746. [CrossRef]

22. Somasundaram, D.; Zhang, F.; Ediriweera, S.; Wang, S.; Li, J.; Zhang, B. Spatial and temporal changes in surface water area of Sri Lanka over a 30-year period. *Remote Sens.* **2020**, *12*, 3701. [CrossRef]

23. Tsuchida, T.; Takeda, S. Is resilience socially emerging or embedded?: A review of "resilience" under climate change in Sri Lanka. *J. Saf. Sci. Resil.* **2021**, *2*, 258–266. [CrossRef]

24. Alahacoon, N.; Edirisinghe, M. Spatial variability of rainfall trends in Sri Lanka from 1989 to 2019 as an indication of climate change. *ISPRS Int. J. Geo-Inf.* **2021**, *10*, 84. [CrossRef]

25. Burt, T.P.; Weerasinghe, K.D. Rainfall distributions in Sri Lanka in time and space: An analysis based on daily rainfall data. *Climate* **2014**, *2*, 242–263. [CrossRef]

26. Eckstein, D.; Künzel, V.; Schäfer, L.; Winges, M. *Global Climate Risk Index*; Germanwatch e.V.: Berlin, Germany, 2020; pp. 1–44. Available online: https://germanwatch.org/sites/germanwatch.org/files/20-2-01e%20Global%20Climate%20Risk%20Index%202020_10.pdf (accessed on 5 January 2022).

27. Cho, H. Climate change risk assessment for Kurunegala, Sri Lanka: Water and heat waves. *Climate* **2020**, *8*, 140. [CrossRef]

28. Naveendrakumar, G.; Vithanage, M.; Kwon, H.H.; Iqbal, M.C.; Pathmarajah, S.; Obeysekara, J. Five decadal trends in averages and extremes of rainfall and temperature in Sri Lanka. *Adv. Meteorol.* **2018**, *2018*, 4217917. [CrossRef]

29. Parajuli, K.; Kang, K. Application of statistical downscaling in GCMs at constructing the map of precipitation in the Mekong River basin. *Russ. Meteorol. Hydrol.* **2014**, *39*, 271–282. [CrossRef]

30. Mahmoodi, N.; Wagner, P.D.; Kiesel, J.; Fohrer, N. Modeling the impact of climate change on streamflow and major hydrological components of an Iranian Wadi system. *J. Water Clim. Chang.* **2021**, *12*, 1598–1613. [CrossRef]

31. Remilekun, A.T.; Thando, N.; Nerhene, D.; Archer, E. Integrated assessment of the influence of climate change on current and future intra-annual water availability in the Vaal River catchment. *J. Water Clim. Chang.* **2021**, *12*, 533–551. [CrossRef]

32. Bao, Z.; Zhang, J.; Yan, X.; Wang, G.; Jin, J.; Liu, Y.; Guan, X. Future streamflow assessment in the Haihe River basin located in northern China using a regionalized variable infiltration capacity model based on 18 CMIP5 GCMs. *J. Water Clim. Chang.* **2020**, *11*, 1551–1569. [CrossRef]

33. Trang, N.T.; Shrestha, S.; Ishidaira, H.; Nhi, P.T. Evaluating the impacts of climate change on the hydrology and water resource availability in the 3S river basin of Cambodia, Laos, and Vietnam. *Vietnam. J. Sci. Technol. Eng.* **2020**, *62*, 77–86. [CrossRef]

34. Ratnayake, U.; Sachindra, D.; Nandalal, K.D. Rainfall forecasting for flood prediction in the Nilwala basin. In *Proceedings of the International Symposium on Coastal Zones and Climate Change: Assessing the Impacts and Developing Adaptation Strategies*; Monash University: Melbourne, Australia, 2010.

35. Acharya, S.C.; Babel, M.; Madsen, H.; Sisomphon, P.; Shrestha, S. Comparison of different quantile regression methods to estimate predictive hydrological uncertainty in the Upper Chao Phraya River Basin, Thailand. *J. Flood Risk Manag.* **2019**, *13*, 1–16. [CrossRef]

36. Piyadasa, R. River sand mining and associated environmental problems in Sri Lanka. In *Sediment Problems and Sediment Management in Asian River Basins*; NHBS Ltd.: Hyderabad, India, 2009; pp. 148–153.

37. De Silva, M.P.; Karunatileka, R.; Thiemann, W.H. Study of some physicochemical properties of Nilwala River waters in Southern Sri Lanka with special reference to effluents resulting from anthropogenic activities. *J. Environ. Sci. Health-Part A Environ. Sci. Eng.* **1998**, *23*, 381–398. [CrossRef]

38. Prabodini, M.K.; Tushara, C.G. *Assessment of Water Quality in the Downstream of Nilwala River*; ACEPS–2013; University of Ruhuna: Galle, Sri Lanka, 2013; pp. 151–158.

39. Elkaduwa, W.K.; Sakthivadivel, R. *Use of Historical Data as a Decision Support Tool in Watershed Management: A Case Study of the Upper Nilwala Basin in Sri Lanka*; IWMI: Colombo, Sri Lanka, 1999. [CrossRef]

40. FAO; IIASA. Harmonized World Soil Database. 2012. Available online: http://webarchive.iiasa.ac.at/Research/LUC/External-World-soil-database/HTML/ (accessed on 3 April 2021).

41. Yatagi, A.; Kamiguchi, K.; Arakawa, O.; Hamada, A.; Yasutomi, N.; Kitoh, A. Constructing a Long-Term Daily Gridded Precipitation Dataset for Asia Based on a Dense Network of Rain Gauges. *Bull. Am. Meteorol. Soc.* **2012**, *93*, 1401–1415.

42. Nguyen, P.; Ombadi, M.; Sorooshian, S.; Hsu, K.; AghaKouchak, A.; Braithwaite, D.; Ashouri, H.; Rose Thorstensen, A. The PERSIANN family of global satellite precipitation data: A review and evaluation of products. *Hydrol. Earth Syst. Sci.* **2018**, *22*, 5801–5816. [CrossRef]

43. Alazzy, A.A.; Lu, H.; Chen, R.; Ali, A.B.; Zhu, Y.; Su, J. Evaluation of satellite precipitation products and their potential influence on hydrological modeling over the Ganzi River Basin of the Tibetan Plateau. *Adv. Meteorol.* **2017**, *2017*, 23. [CrossRef]

44. Zam, P.; Shrestha, S.; Budhathoki, A. Assessment of climate change impact on hydrology of a transboundary river of Bhutan and India. *J. Water Clim. Chang.* **2021**, *12*, 3224–3239. [CrossRef]

45. Jet Propulsion Labrotory 2021. Available online: https://asterweb.jpl.nasa.gov/gdem.asp (accessed on 21 April 2021).

46. Yin, Z.; Feng, Q.; Yang, L.; Wen, X.; Si, J.; Zou, S. Long term quantification of climate and land cover change impacts on streamflow in an Alpine River Catchment, Northwestern China. *Sustainability* **2017**, *9*, 1278. [CrossRef]

47. Immerzee, W.W. *Bias Correction for Satellite Precipitation Estimation Used by the MRC Mekong Flood Forecasting System*; Mekong River Commission: Wageningen, The Netherlands, 2010.

48. Chen, J.; Fang, X.; Wen, Z.; Chen, Q.; Ma, M.; Huang, Y.; Yang, L. Spatio-temporal patterns and impacts of sediment variations in downstream of the Three Gorges Dam on the Yangtze River, China. *Sustainability* **2018**, *10*, 93. [CrossRef]

49. Zango, B.S.; Seidou, O.; Sartaj, M.; Nakhaei, N.; Stiles, K. Impacts of urbanization and climate change on water quantity and quality in the Carp River watershed. *J. Water Clim. Chang.* **2022**, *13*, 786–816. [CrossRef]

50. Usman, M.; Pan, X.; Penna, D.; Ahmad, B. Hydrologic alteration and potential ecosystemic implications under a changing climate in the Chitral River, Hindukush region, Pakistan. *J. Water Clim. Chang.* **2021**, *12*, 1471–1486. [CrossRef]

51. Sidiqi, M.; Shrestha, S. Assessment of climate change impact on the hydrology of the Kabul River Basin, Afghanistan. *J. Water Eng. Manag.* **2021**, *2*, 1–21. [CrossRef]

52. Bekele, W.T.; Haile, A.T.; Rientjes, T. Impact of climate change on the stream flow of the Arjo-Didessa catchment under RCP scenarios. *J. Water Clim. Chang.* **2021**, *12*, 2325–2337. [CrossRef]

53. Bhatta, B.; Shrestha, S.; Shrestha, P.K.; Talchabhadel, R. Evaluation and application of a SWAT model to assess the climate change impact on the hydrology of the Himalayan River Basin. *Catena* **2019**, *181*, 13. [CrossRef]

54. Shrestha, A.; Shrestha, S.; Tingsanchali, T.; Budhathoki, A.; Ninsawat, S. Adapting hydropower production to climate change: A case study of Kulekhani Hydropower Project in Nepal. *J. Clean. Prod.* **2021**, *279*, 1–14. [CrossRef]

55. Adham, M.I.; Shirazi, S.M.; Othman, F.; Rahman, S.; Yusop, Z.; Ismail, Z. Runoff potentiality of a watershed through SCS and functional data analysis technique. *Sci. World J.* **2014**, *2014*, 1–15. [CrossRef] [PubMed]

56. Kim, Y.; Yu, J.; Lee, K.; Chung, H.; Sung, H.; Jeon, S. Impact assessment of climate change on the near and the far future streamflow in the Bocheongcheon Basin of Geumgang river, South Korea. *Water* **2021**, *13*, 2516. [CrossRef]

57. Gunathilake, M.B.; Karunanayake, C.; Gunathilake, A.S.; Marasingha, N.; Samarasinghe, J.T.; Bandara, I.M.; Rathnayake, U. Hydrological models and Artificial Neural Networks (ANNs) to simulate streamflow in a tropical catchment of Sri Lanka. *Appl. Comput. Intell. Soft Comput.* **2021**, *2021*, 1–9. [CrossRef]

58. Shekar, N.C.; Vinay, D.C. Performance of HEC-HMS and SWAT to simulate streamflow in the sub-humid tropical Hemavathi catchment. *J. Water Clim. Chang.* **2021**, *12*, 1–13. [CrossRef]

59. Yang, S.C.; Yang, T.H. Uncertainty assessment: Reservoir inflow forecasting with ensemble precipitation forecasts and HEC-HMS. *Adv. Meteorol.* **2014**, *2014*, 1–11. [CrossRef]

60. Habibu, I.; Kamal, M.R.; Hin, L.S.; Abdullah, A.F. Performance of HEC-HMS and ArcSWAT models for assessing climate change impacts on streamflow at Bernam River Basin in Malaysia. *Pertanika J. Sci. Technol.* **2020**, *28*, 1027–1048.

61. Sharafati, A.; Khazaei, M.R.; Nashwan, M.S.; Al-Ansari, N.; Yaseen, Z.M.; Shahid, S. Assessing the uncertainty associated with flood features due to variability of rainfall and hydrological parameters. *Adv. Civ. Eng.* **2020**, *2020*, 1–9. [CrossRef]

62. Shrestha, S.; Bajracharya, A.R.; Babel, M.S. Assessment of risks due to climate change for the Upper Tamakoshi hydropower project in Nepal. *Clim. Risk Manag.* **2016**, *14*, 27–41. [CrossRef]

63. Foster, H.E. Duration Curves. *Trans. ASCE* **1934**, *99*, 1213–1267. [CrossRef]

64. Vogel, R.R.; Fennessey, N.W. Flow-duration curve. I: New interpretation and confidence intervals. *J. Water Resour. Plan. Manag.* **1994**, *120*, 485–504. [CrossRef]

65. Swain, J.B.; Patra, K.C. Impact assessment of land use/land cover and climate change on streamflow regionalization in an ungauged catchment. *J. Water Clim. Chang.* **2019**, *10*, 554–568. [CrossRef]

66. Budhathoki, A.; Babel, M.S.; Shrestha, S.; Meon, G.; Kamalamma, A.G. Climate change impact on water balance and hydrological extremes in different physiographic regions of the West Seti River Basin, Nepal. *Ecohydrol. Hydrobiol.* **2020**, *21*, 79–95. [CrossRef]

67. Moriasi, D.N.; Arnold, J.G.; Van Liew, M.W.; Bingner, R.L.; Harmel, R.D.; Veith, T.L. Model Evaluation Guidelines for Systematic Quantification of Accuracy in Watershed Simulations. *Trans. ASABE* **2007**, *50*, 885–900. [CrossRef]

68. Babel, M.S.; Gunathilake, M.B.; Jha, M.K. Evaluation of Ecosystem-Based Adaptation Measures for Sediment Yield in a Tropical Watershed in Thailand. *Water* **2021**, *13*, 2767. [CrossRef]

69. Gunathilake, M.B.; Zamri, M.N.M.; Alagiyawanna, T.P.; Samarasinghe, J.T.; Baddewela, P.K.; Babel, M.S.; Jha, M.K.; Rathnayake, U.S. Hydrologic Utility of Satellite-Based and Gauge-Based Gridded Precipitation Products in the Huai Bang Sai Watershed of Northeastern Thailand. *Hydrology* **2021**, *8*, 165. [CrossRef]

70. Asghar, A.; Ali Amin, J.; Ribbe, L. Integrated hydrological modeling for assessment of water demand and supply under socio-economic and IPCC climate change scenarios using WEAP in Central Indus Basin. *J. Water Supply Res. Technol.* **2019**, *68*, 136–148. [CrossRef]

71. Zhang, M.; Zhang, J.; Song, Y. Preliminary Research and Application of MIKE SHE Model in Jialingjiang River Basin. *IOP Conf. Ser. Earth Environ. Sci.* **2019**, *304*, 022088. [CrossRef]

72. Ghaderpour, E. JUST: MATLAB and Python software for change detection and time series analysis. *GPS Solut.* **2021**, *25*, 1–7. [CrossRef]

73. Ghaderpour, E.; Pagiatakis, S.D. LSWAVE: A MATLAB software for the least-squares wavelet and cross-wavelet analyses. *GPS Solut.* **2019**, *23*, 1–8. [CrossRef]